SLAC – PUB – 3957
May 1986
(A)

OPTICS MODULES FOR CIRCULAR ACCELERATOR DESIGN*

Karl L. Brown
Stanford Linear Accelerator Center, Stanford University, Stanford, CA 94305

and

Roger V. Servranckx
University of Saskatchewan, Saskatoon, Saskatchewan, Canada S7N-0W0

1 INTRODUCTION AND SUMMARY

This paper is intended as a companion paper to 'Circular Machine Design Techniques and Tools' presented at this conference by Roger Servranckx. The intent here is to provide a tutorial discussion on the basic optics of circular particle accelerators for the benefit of those readers who have a fundamental knowledge of charged particle optics but do not make it their profession to design particle accelerators.

We begin the tutorial by presenting the solutions of the first-order differential equations of motion for a single particle in a closed circular machine introducing the concepts of phase shift, beta functions, and the Courant-Snyder invariant. From these solutions we derive the transfer matrix between two points in the machine as a function of the phase shift and the parameters contained in the Courant-Snyder invariant.

We then introduce typical optical building blocks (modules) used in circular machine designs and relate them to their characteristic transfer matrix elements, the phase shift through them, and the Courant-Snyder-Twiss parameters, β, α, and γ.

Next we discuss the systematics of some elementary phase ellipse matching problems between optical modules.

* Work supported in part by the Department of Energy, contract DE-AC03-76SF00515 and by the National Sciences and Engineering Research Council of Canada.

Presented at the Second International Conference on Charged Optics, Albuquerque, New Mexico, May 19-23, 1986

The report ends with a discussion of second-order optical modules and how they are used to provide the momentum bandwidth needed for the design of a typical circular machine.

2 FIRST-ORDER OPTICS

2.1 Notations and Definitions

As in TRANSPORT,[1][2][3] we represent the position and direction of travel of a particle via a six-dimensional vector:

$$X = \begin{pmatrix} x_1 \\ x_2 \\ x_3 \\ x_4 \\ x_5 \\ x_6 \end{pmatrix} = \begin{pmatrix} x \\ x' \\ y \\ y' \\ l \\ \delta \end{pmatrix}$$

The coordinates x and y represent, respectively, the horizontal and vertical displacements at the position of the particle, and x' and y' represent the slopes of the projection of the trajectory in the same planes. The quantity l represents the longitudinal position of the particle relative to a particle travelling on the reference trajectory with the reference momentum. The last coordinate $\delta = (p - p_0)/p_0$ gives the fractional deviation of the momentum of the particle from the central design momentum of the system.

In first-order optics, the motion is described by the following matrix equation:

$$x_i = \sum_{j=1}^{6} R_{ij} x_{0j} \ , \qquad i = 1, 2, \ldots, 6 \tag{2.1}$$

Equation (2.1) can also be rewritten in compact matrix notation as

$$X = RX_0 \ .$$

In optics studies it is customary first to study the properties of a set of optical elements by restricting the momentum of the test particles to one value (called the reference momentum), and then to study the properties as the momentum is changed. The elements R_{ij} of the matrix R that contain one subscript with the value 6 are called chromatic terms. The elements R_{ij} for which no subscript is equal to 6 are referred to as geometric terms.

If midplane symmetry is applicable, then the R matrix has the following decoupled form :

$$R = \begin{pmatrix} c_x(s) & s_x(s) & 0 & 0 & 0 & d_x(s) \\ c_x'(s) & s_x'(s) & 0 & 0 & 0 & d_x'(s) \\ 0 & 0 & c_y(s) & s_y(s) & 0 & 0 \\ 0 & 0 & c_y'(s) & s_y'(s) & 0 & 0 \\ R_{51} & R_{52} & R_{53} & R_{54} & R_{55} & R_{56} \\ R_{61} & R_{62} & R_{63} & R_{64} & R_{65} & R_{66} \end{pmatrix} .$$

2.2 Single-Particle Linear Optics for a Closed Machine

The first-order equations of motions, in a circular machine, are given by[2]

$$\frac{d^2x}{ds^2} + k_x^2(s)x = \frac{\Delta p/p}{\rho(s)} = \delta h(s) ,$$

$$\frac{d^2y}{ds^2} + k_y^2(s)y = 0 ,$$

$$\text{where} \qquad \delta = \Delta p/p .$$

In a closed machine the functions $k_x(s)$,$k_y(s)$ and $\rho(s)$ are periodic functions of s with the period L, where L is the length of the closed orbit in the circular machine. Let us consider solutions for the nondispersive ($\delta = 0$) stable case. The theorem of Floquet (see Ref. 4) states that there exist two functions $\beta(s)$ (periodic) and $\psi(s)$ in terms of which the general solution $x(s)$ can be expressed. For the x phase plane the result is:

$$x(s) = \sqrt{\epsilon\beta(s)}\cos(\psi(s) + \phi)$$

where ϵ and ϕ are two arbitrary constants and the two functions $\beta(s)$ and $\psi(s)$ are not independent, but are linked by the simple relation

$$\psi(s) = \int_0^s \frac{d\tau}{\beta(\tau)} .$$

$\psi(s)$ is called the "machine phase shift" between points 0 and s. Differentiation of $x(\mathrm{s})$ with respect to s yields

$$x'(\mathrm{s}) = \sqrt{\frac{\epsilon}{\beta(\mathrm{s})}}\frac{\beta'(\mathrm{s})}{2}\cos(\psi(\mathrm{s})+\phi) - \sqrt{\epsilon\beta(\mathrm{s})}(\sin(\psi(\mathrm{s})+\phi)\frac{1}{\beta(\mathrm{s})})$$

$$= -\sqrt{\frac{\epsilon}{\beta(\mathrm{s})}}\Big(\alpha(\mathrm{s})\cos(\psi(\mathrm{s})+\phi) + \sin(\psi(\mathrm{s})+\phi)\Big)$$

where we now define the function $\alpha(\mathrm{s})$ by

$$\beta'(\mathrm{s}) = -2\alpha(\mathrm{s}) \ .$$

Alternatively $x'(\mathrm{s})$ can be written in the form

$$x'(\mathrm{s}) = \sqrt{\epsilon\gamma(\mathrm{s})}\cos(\chi(\mathrm{s})+\phi)$$

where $\chi(\mathrm{s})$ satisfies the relation

$$\tan(\psi(\mathrm{s}) - \chi(\mathrm{s})) = \frac{1}{\alpha(\mathrm{s})}$$

or equivalently

$$\sin(\psi(\mathrm{s}) - \chi(\mathrm{s})) = -\frac{1}{\sqrt{\beta(\mathrm{s})\gamma(\mathrm{s})}}$$

and the function $\gamma(\mathrm{s})$ is defined by

$$\gamma(\mathrm{s}) = \frac{1+\alpha(\mathrm{s})^2}{\beta(\mathrm{s})} \ .$$

The functions $\beta(\mathrm{s})$, $\alpha(\mathrm{s})$, and $\gamma(\mathrm{s})$ are all periodic with the period L, where L is the length of the closed machine. Consider the values of the solution for x and its derivative at successive revolutions at a fixed point s. We can describe the motion at position s by plotting the values of x and x' in the "x-phase plane". Eliminating the trigonometric functions from the expressions of $x(\mathrm{s})$ and $x'(\mathrm{s})$ yields, after some manipulation, the 'Courant-Snyder' invariant[5] (the equation of the machine ellipse). The result is:

$$\gamma(\mathrm{s})x^2 + 2\alpha(\mathrm{s})xx' + \beta(\mathrm{s})x'^2 = \epsilon \ ,$$

which shows that the positions (x, x') of a particle at the coordinate s upon successive turns lie on an ellipse. The parameters α, β, and γ are sometimes referred to, in the literature, as the Twiss parameters.[6] Similar equations may be derived for the y, y' phase plane. We assume, in this discussion, that midplane symmetry is applicable and therefore there is no linear coupling between the x and y phase planes.

2.2.1 *The Machine Ellipse*

This 'machine ellipse' may also be represented in a matrix form as follows:

$$T = \begin{pmatrix} \beta(\mathrm{s}) & -\alpha(\mathrm{s}) \\ -\alpha(\mathrm{s}) & \gamma(\mathrm{s}) \end{pmatrix} \tag{2.2}$$

where T has a determinant equal to 1. The equation of the ellipse characteristic of the machine may then be written in the matrix form

$$X^t T^{-1} X = \epsilon \qquad \text{where} \qquad X = \begin{pmatrix} x \\ x' \end{pmatrix} \tag{2.3}$$

The area of the ellipse is $\pi\epsilon$. We can compute the maximum x excursion x_{max} and the maximum x' excursion x'_{max}. They are given by the expressions:

$$x_{\mathrm{max}} = \sqrt{\beta\epsilon} \qquad , \qquad x'_{\mathrm{max}} = \sqrt{\gamma\epsilon}\ .$$

From the explicit equation of the ellipse one can also obtain the coordinates of the intercepts with the axes:

$$x_{\mathrm{inter}} = \sqrt{\frac{\epsilon}{\gamma}} \qquad , \qquad x'_{\mathrm{inter}} = \sqrt{\frac{\epsilon}{\beta}}\ .$$

and from these expressions one can deduce alternative expressions for the area of the ellipse:

$$\text{Area} = \pi\epsilon = \pi x_{\mathrm{max}} x'_{\mathrm{inter}} = \pi x_{\mathrm{inter}} x'_{\mathrm{max}}\ .$$

This result can be generalized to dimension n. For n dimensions ϵ is the product of one intercept, one maximum and $(n-2)$ maxima of subspace intercepts. Figure 1 illustrates these points in two dimensions.

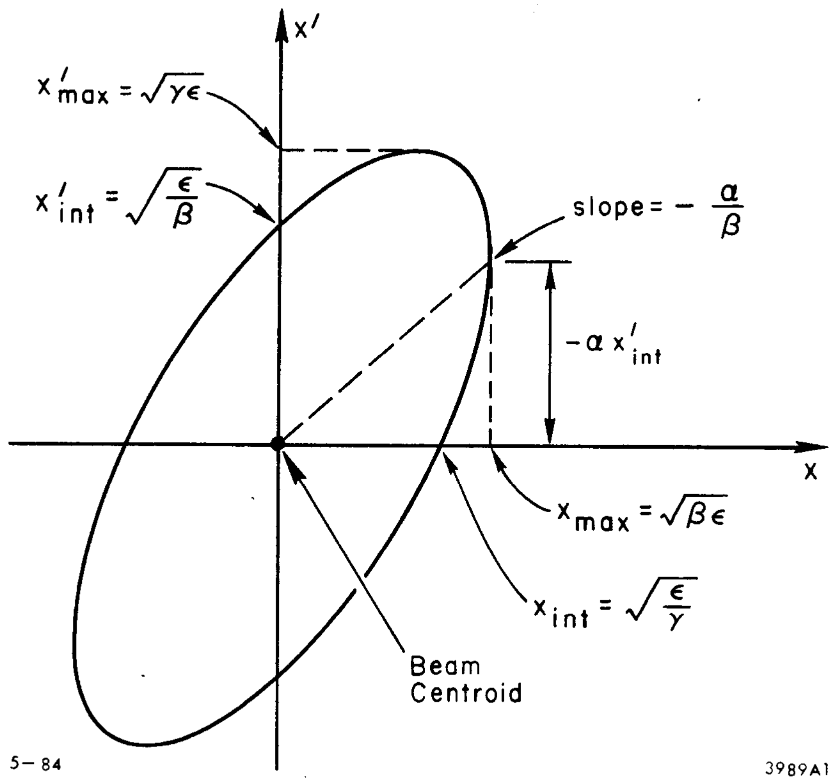

Fig. 1. An Ellipse based on the Machine Parameters β, α, γ, illustrating single-particle motion in a closed machine. The area of the ellipse is $A = \pi\epsilon$.

Consider now two points S_1 and S_2 on the reference orbit of the closed machine. Let T_1 and T_2 denote the machine ellipse matrices at these two points and R the optical transfer matrix from point S_1 to point S_2. Similar to the beam ellipses in TRANSPORT,[2][3] we have the following transformation relating T_2 to T_1:

$$T_2 = RT_1R^t$$

or

$$\begin{pmatrix} \beta_2 \\ \alpha_2 \\ \gamma_2 \end{pmatrix} = \begin{pmatrix} R_{11}^2 & -2R_{11}R_{12} & R_{12}^2 \\ -R_{11}R_{21} & 1+2R_{12}R_{21} & -R_{12}R_{22} \\ R_{21}^2 & -2R_{21}R_{22} & R_{22}^2 \end{pmatrix} \begin{pmatrix} \beta_1 \\ \alpha_1 \\ \gamma_1 \end{pmatrix} . \qquad (2.4)$$

2.3 The Relationship Between the Beam Ellipse and the Machine Ellipse

Consider a closed machine that is characterized by the ellipse E_1 with emittance ϵ and area A_1, as shown in Fig. 2. Let P_1 denote a point on that ellipse and let O denote the origin of the axes. After successive turns around the machine the point P_1 will reappear at P_2, P_3, etc.

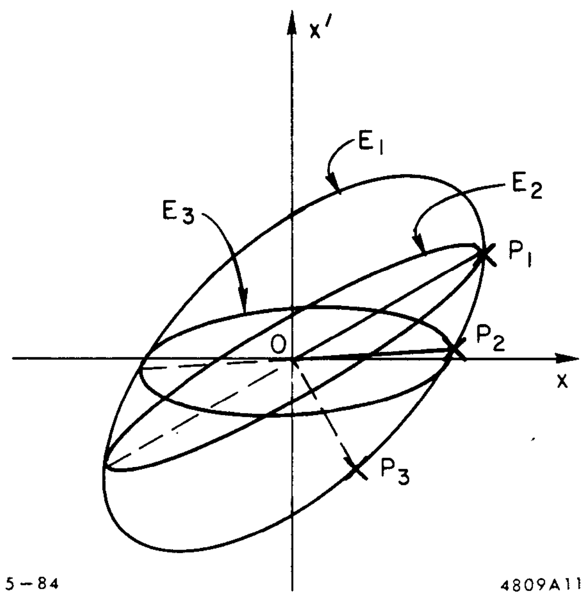

Fig. 2. The Superposition of *Beam* Ellipses E_2 and E_3 with a *Machine* Ellipse E_1.

Consider now an ellipse E_2 inscribed in E_1 with a contact point at P_1. Let the ellipse E_2 represent a beam of particles circulating in the machine. Ellipse E_2 becomes, after one turn, ellipse E_3 with contact point P_2. Ellipses E_2 and E_3 have the same area.

When the beam ellipse E_2 is concentric and similar to the machine ellipse E_1, the beam is said to be **matched** to the machine. In this instance the beam reappears on successive turns as the same ellipse, but the individual particles in the beam rotate around the ellipse as did the points P_1 etc.

Let us find the transfer matrix which transforms the machine ellipse defined by the input values β_1 and α_1 at position s_1 into an ellipse with the values β_2 and α_2 at position s_2.

Consider again the solutions as given by the Floquet theorem:

$$x(\mathrm{s}) = \sqrt{\epsilon\beta(\mathrm{s})}\cos(\psi(\mathrm{s}) + \phi) \ ,$$

$$x'(\mathrm{s}) = -\sqrt{\frac{\epsilon}{\beta(\mathrm{s})}}\Big(\alpha(\mathrm{s})\cos(\psi(\mathrm{s}) + \phi) + \sin(\psi(\mathrm{s}) + \phi)\Big) \ .$$

Expanding the trigonometric functions and simplifying the notation gives

$$x = \sqrt{\epsilon\beta}(\cos\psi\cos\phi - \sin\psi\sin\phi) \ ,$$

$$x' = -\sqrt{\frac{\epsilon}{\beta}}(\alpha\cos\psi\cos\phi - \alpha\sin\psi\sin\phi + \sin\psi\cos\phi + \cos\psi\sin\phi) \ .$$

The point having $\psi = 0$ is assumed to be associated with the values β_1 and α_1 and x_1 and x_1'; these values then satisfy the following relations:

$$x_1 = \sqrt{\epsilon\beta_1}\cos\phi \ ,$$

$$x_1' = -\sqrt{\frac{\epsilon}{\beta_1}}(\alpha_1\cos\phi + \sin\phi) \ .$$

Denoting by β_2, α_2, x_2, and x'_2 the values associated with ψ nonzero, and eliminating $\cos\phi$ and $\sin\phi$ from the previous four equations, one gets

$$x_2 = x_1\sqrt{\frac{\beta_2}{\beta_1}}(\cos\psi + \alpha_1\sin\psi) + x_1'\sqrt{\beta_2\beta_1}\sin\psi \ ,$$

$$x_2' = x_1\frac{-\alpha_2\cos\psi - \sin\psi - \alpha_2\alpha_1\sin\psi + \alpha_1\cos\psi}{\sqrt{\beta_2\beta_1}} + x_1'\sqrt{\frac{\beta_1}{\beta_2}}(\cos\psi - \alpha_2\sin\psi) \ .$$

From the above equations we deduce the transfer matrix between position 1 and position 2 to be

$$R = \begin{pmatrix} \sqrt{\frac{\beta_2}{\beta_1}}(\cos\Delta\psi + \alpha_1\sin\Delta\psi) & \sqrt{\beta_1\beta_2}\sin\Delta\psi \\ -\frac{(1+\alpha_1\alpha_2)\sin\Delta\psi + (\alpha_2 - \alpha_1)\cos\Delta\psi}{\sqrt{\beta_1\beta_2}} & \sqrt{\frac{\beta_1}{\beta_2}}(\cos\Delta\psi - \alpha_2\sin\Delta\psi) \end{pmatrix} \tag{2.5}$$

where $\Delta\psi$ is the phase shift between position s_1 and s_2.

In the particular case where the input values (β_1, α_1) are equal to the output values (β_2, α_2) the transfer matrix becomes

$$R = \begin{pmatrix} \cos\mu + \alpha\sin\mu & \beta\sin\mu \\ -\gamma\sin\mu & \cos\mu - \alpha\sin\mu \end{pmatrix} \tag{2.6}$$

where we have defined

$$\beta = \beta_1 = \beta_2 \ , \qquad \alpha = \alpha_1 = \alpha_2 \ , \qquad \mu = \Delta\psi \ ,$$

and

$$\gamma = \frac{1+\alpha^2}{\beta} \ .$$

Formula (2.5) expresses the elements of the transfer matrix R in terms of the input parameters β_1, α_1, the output parameters β_2, α_2, and the phase advance $\Delta\psi$ between positions s_1 and s_2.

The linearised stable motion around the reference closed orbit of a circular machine can always be expressed by the matrix formula (2.6).

It is also possible to express the output Twiss parameters and the phase advance in terms of the input Twiss parameters and the matrix elements. The first part of this *inversion* process is achieved in formula (2.4) which we reproduce here:

$$\begin{pmatrix} \beta_2 \\ \alpha_2 \\ \gamma_2 \end{pmatrix} = \begin{pmatrix} R_{11}^2 & -2R_{11}R_{12} & R_{12}^2 \\ -R_{11}R_{21} & 1+2R_{12}R_{21} & -R_{12}R_{22} \\ R_{21}^2 & -2R_{21}R_{22} & R_{22}^2 \end{pmatrix} \begin{pmatrix} \beta_1 \\ \alpha_1 \\ \gamma_1 \end{pmatrix} \ . \tag{2.7}$$

The phase shift $\Delta\psi$ is derived from formula (2.5) as

$$\tan\Delta\psi = \frac{R_{12}}{R_{11}\beta_1 - R_{12}\alpha_1} \tag{2.8}$$

or

$$\sin\Delta\psi = \frac{R_{12}}{\sqrt{\beta_1\beta_2}} \tag{2.9}$$

or equivalently by the formulas relating $\psi(s)$ and $\beta(s)$:

$$\Delta\psi = \int_{s_1}^{s_2} \frac{ds}{\beta(s)} \ .$$

Let us look at some elementary configurations and determine their phase shifts:

a) A thin lens is characterized by $s_1 = s_2$ so that $\Delta\psi = 0$.

b) If $R_{12} = 0$ (point to point imaging) then $\Delta\psi = n\pi$.

c) If $R_{11} = 0$ (parallel to point imaging) then $\tan\Delta\psi = -1/\alpha_1$.

d) For a drift of length L, $R_{12} = L$ and $\sin\Delta\psi = L/\sqrt{\beta_1\beta_2}$.

It is perhaps worthwhile to comment on the meaning of 'phase shift' in a circular machine.

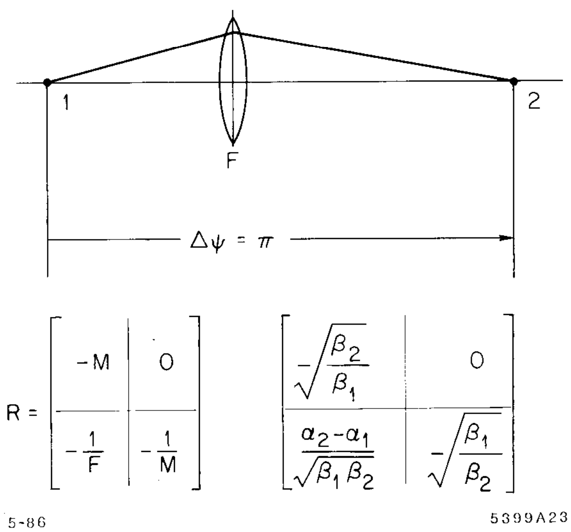

Fig. 3 Phase Shift for Point to Point Imaging

Consider Fig. 3 where we show a single lens imaging from point 1 to point 2. This corresponds to the matrix element $R_{12} = 0$. From the figure and Eq. (2.5) we can conclude that the phase shift is π. In this case we only need to know that $R_{12} = 0$ in order to conclude that the phase shift is zero or $n\pi$. With the further information contained in Fig. 3 we know that the answer is π. No additional information about the incoming phase ellipse is necessary.

Now, in contrast, consider Fig. 4 where again we have a single lens but with the matrix element $R_{11} = 0$. This corresponds to parallel to point imaging.

Comparing again with Eq. (2.5), we discover that we need to know the orientation of the incoming phase ellipse, α_1, at the entrance of the module in order to evaluate the phase shift through the module.

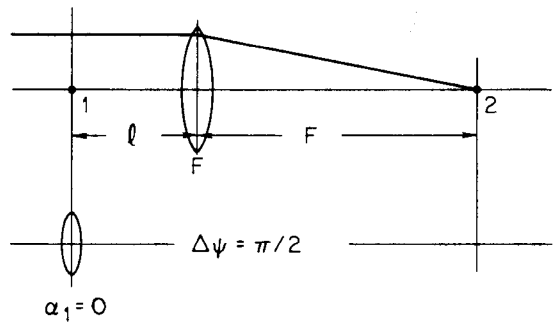

$$R = \begin{bmatrix} 0 & F \\ -\frac{1}{F} & \left(1-\frac{\ell}{F}\right) \end{bmatrix} = \begin{bmatrix} 0 & \sqrt{\beta_1\beta_2} \\ -\frac{1}{\sqrt{\beta_1\beta_2}} & -\alpha_2\sqrt{\frac{\beta_1}{\beta_2}} \end{bmatrix}$$

5-86 5399A22

Fig. 4 Phase Shift for Parallel to Point Imaging

If $\alpha_1 = 0$, corresponding to an upright ellipse, then the phase shift is

$$\Delta\psi = \frac{\pi}{2}$$

otherwise

$$\tan(\Delta\psi) = -\frac{1}{\alpha_1}$$

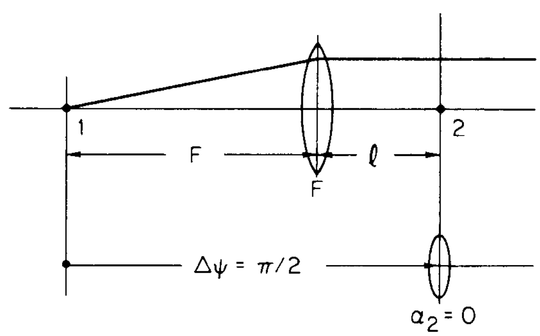

$$R = \begin{bmatrix} \left(1-\frac{\ell}{F}\right) & F \\ -\frac{1}{F} & 0 \end{bmatrix} = \begin{bmatrix} \alpha_1\sqrt{\frac{\beta_2}{\beta_1}} & \sqrt{\beta_1\beta_2} \\ -\frac{1}{\sqrt{\beta_1\beta_2}} & 0 \end{bmatrix}$$

5-86
5399A21

Fig. 5 Phase Shift for Point to Parallel Imaging

As a third example consider Fig. 5 where $R_{22} = 0$, corresponding to point to parallel imaging. In this case we readily conclude that we must have a knowledge of the orientation, α_2, of the machine ellipse at the endpoint of the module in order to determine the phase shift through the module. Here we find that if $\alpha_2 = 0$ (an upright ellipse) then

$$\Delta\psi = \frac{\pi}{2}$$

otherwise

$$\tan(\Delta\psi) = \frac{1}{\alpha_2}$$

In more complex modules, such as a FODO array, to be discussed later, it will be seen that it is often necessary to know both β and α at either the beginning or the end of the module, in addition to the transfer matrix, in order to deduce the phase shift through the module. This can be seen by inspection of Eq. (2.8).

3 OPTICAL BUILDING BLOCKS

We shall now turn our attention to the study of special elements or sets of elements which can be used to design optics modules for particle accelerators.

3.0.1 A Drift Space or Field-Free Region

The transfer matrix of a drift is

$$R = \begin{pmatrix} 1 & L \\ 0 & 1 \end{pmatrix}$$

from which one derives

$$\Delta x = x_2 - x_1 = L x_1{}' \qquad \text{and} \qquad x_2{}' = x_1{}' = \text{a constant} .$$

The Twiss parameters transform as follows according to formula (2.7):

$$\begin{pmatrix} \beta_2 \\ \alpha_2 \\ \gamma_2 \end{pmatrix} = \begin{pmatrix} 1 & -2L & L^2 \\ 0 & 1 & -L \\ 0 & 0 & 1 \end{pmatrix} \begin{pmatrix} \beta_1 \\ \alpha_1 \\ \gamma_1 \end{pmatrix}$$

From this relation one obtains

$$\Delta\alpha = \alpha_2 - \alpha_1 = -L\gamma_1 \qquad \text{and} \qquad \gamma_2 = \gamma_1 = \text{ a constant} .$$

The relation (2.9) applied to the drift gives

$$\sin\Delta\psi = \frac{R_{12}}{\sqrt{\beta_1\beta_2}} = \frac{L}{\sqrt{\beta_1\beta_2}}$$

showing the relation between the phase advance and the length. The relation

(2.8) gives

$$\tan \Delta\psi = \frac{R_{12}}{R_{11}\beta_1 - R_{12}\alpha_1} = \frac{L}{\beta_1 - L\alpha_1} \ .$$

Consider the extreme point on the beam ellipse shown in Fig. 6.

As the beam travels through the drift space, this point will be displaced by Δx given by

$$\Delta x = L\sqrt{\gamma\epsilon} = L\sqrt{\frac{\epsilon}{\beta_w}}$$

where β_w is the β value achieved at the point where the beam has a waist.

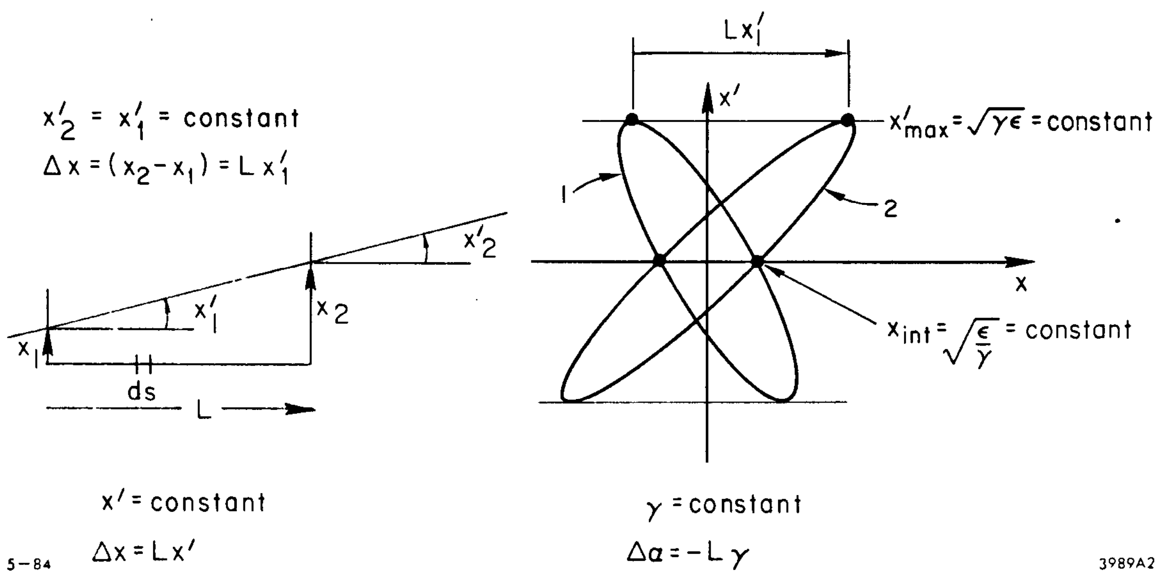

Fig. 6. The Transformation of an Ellipse through a Drift (Field-free) Space.

3.0.2 A Thin Lens

A focusing thin lens has the following transfer matrix:

$$R = \begin{pmatrix} 1 & 0 \\ -1/F & 1 \end{pmatrix}$$

from which one derives

$$x_2 = x_1 = \text{a constant} \qquad \text{and} \qquad \Delta x' = x_2{}' - x_1{}' = -\frac{x_1}{F} \ .$$

The Twiss parameters transform according to formula (2.7),

$$\begin{pmatrix} \beta_2 \\ \alpha_2 \\ \gamma_2 \end{pmatrix} = \begin{pmatrix} 1 & 0 & 0 \\ 1/F & 1 & 0 \\ 1/F^2 & 2/F & 1 \end{pmatrix} \begin{pmatrix} \beta_1 \\ \alpha_1 \\ \gamma_1 \end{pmatrix}$$

which gives

$$\beta_2 = \beta_1 = \text{a constant} \qquad \text{and} \qquad \Delta\alpha = \alpha_2 - \alpha_1 = \frac{\beta_1}{F} \ .$$

The relation (2.8) gives

$$\tan \Delta\psi = \frac{R_{12}}{R_{11}\beta_1 - R_{12}\alpha_1} = 0$$

and so $\Delta\psi = 0$ because the integral

$$\Delta\psi = \int \frac{ds}{\beta(s)} = 0$$

since the thin lens has a length equal to zero. The transformation of an ellipse through a focusing thin lens is illustrated in Fig. 7.

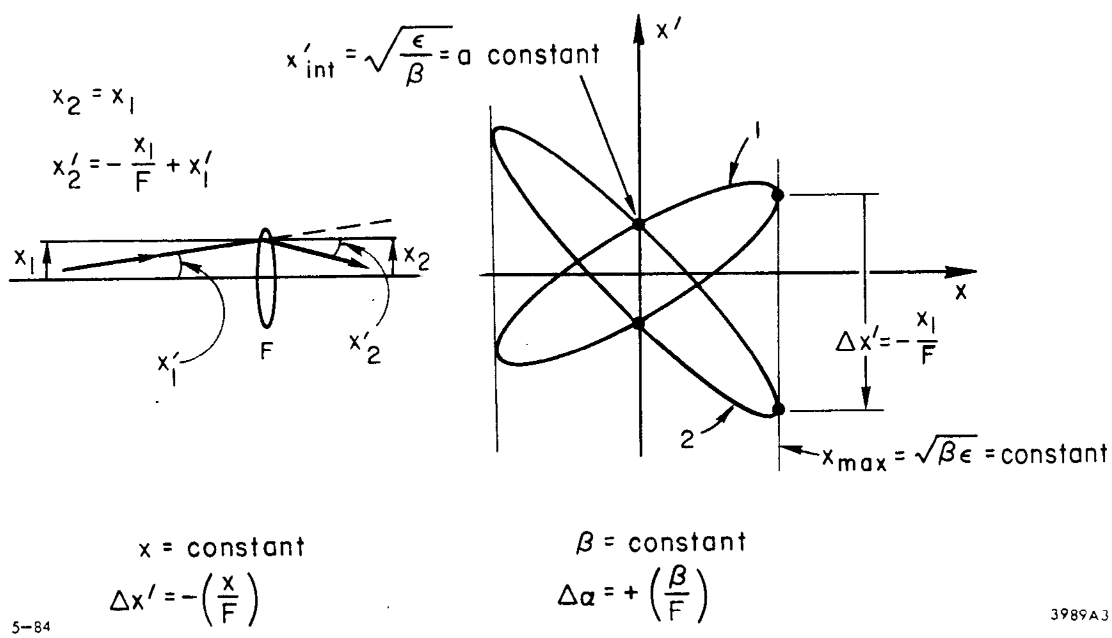

Fig. 7. The Transformation of an Ellipse through a Focusing *Thin* Lens.

3.0.3 A Quadrupole

The thin lens quadrupole behaves in each phase plane (x, x') and (y, y') like a thin lens of opposite signs. If the lens is focusing in the x-plane, the matrices can be written as follows:

$$R = \begin{pmatrix} 1 & 0 \\ \mp 1/F & 1 \end{pmatrix} .$$

We have assumed here that the quantity F is positive.

The phase advance is zero in both planes, and β is constant in both planes. The change in α is given by

$$\Delta\alpha = \pm\frac{\beta}{F} .$$

In these expressions the upper sign applies to the (x, x') focusing plane and the lower sign to the (y, y') defocusing plane.

3.0.4 A thin Dipole

A wedge dipole with the field index n equal to 0 (i.e. a uniform field) can be simulated as a thin element (having zero length), located at its middle, and having the following transfer matrix:

$$R = \begin{pmatrix} 1 & 0 & 0 \\ -\sin\alpha/\rho & 1 & \sin\alpha \\ 0 & 0 & 1 \end{pmatrix}$$

where α is the deflection angle of the central trajectory and where the third row and column describe the part of the transformation associated with the energy-dependent parameter $\delta = (\Delta p/p)$. The wedge dipole behaves like a thin lens of focal length $F = \rho/\sin\alpha$ in the (x, x') plane. In the (y, y') plane the wedge dipole behaves like a drift for a sharp cutoff field boundary. The matrix R gives us

$$x_2 = x_1 = \text{a constant} \qquad \text{and} \qquad \Delta x' = x_2{}' - x_1{}' = -\frac{x_1 \sin\alpha}{\rho} + \delta\sin\alpha .$$

The formula (2.7) becomes

$$\begin{pmatrix} \beta_2 \\ \alpha_2 \\ \gamma_2 \end{pmatrix} = \begin{pmatrix} 1 & 0 & 0 \\ \sin\alpha/\rho & 1 & 0 \\ \sin^2\alpha/\rho^2 & 2\sin\alpha/\rho & 1 \end{pmatrix} \begin{pmatrix} \beta_1 \\ \alpha_1 \\ \gamma_1 \end{pmatrix}$$

which gives

$$\beta_2 = \beta_1 = \text{a constant} \qquad \text{and} \qquad \Delta\alpha = \alpha_2 - \alpha_1 = \frac{\beta_1 \sin\alpha}{\rho} \ .$$

As for the thin lens, the relation (2.9) shows that $\Delta\psi = 0$ for the zero length dipole.

3.1 Study of Simple Useful Composite Modules

Using the basic elements discussed in the previous section we shall now explore some typical composite modules.

3.1.1 Basic Focusing Module

If a focusing thin lens of focal length F is placed between two drifts of length F, the transfer matrix for the composite system is

$$R = \begin{pmatrix} 1 & F \\ 0 & 1 \end{pmatrix} \begin{pmatrix} 1 & 0 \\ -1/F & 1 \end{pmatrix} \begin{pmatrix} 1 & F \\ 0 & 1 \end{pmatrix}$$
$$= \begin{pmatrix} 0 & F \\ -1/F & 0 \end{pmatrix} \ .$$

From the matrix R we observe that angles are transformed to displacements and displacements to angles as follows:

$$x_2 = F x_1{}' \qquad \text{and} \qquad x_2{}' = -\frac{x_1}{F} \ .$$

From the relation (2.7) we have

$$\begin{pmatrix} \beta_2 \\ \alpha_2 \\ \gamma_2 \end{pmatrix} = \begin{pmatrix} 0 & 0 & F^2 \\ 0 & -1 & 0 \\ 1/F^2 & 0 & 0 \end{pmatrix} \begin{pmatrix} \beta_1 \\ \alpha_1 \\ \gamma_1 \end{pmatrix}$$

from which

$$\beta_2 = F^2 \gamma_1 \qquad \text{and} \qquad \alpha_2 = -\alpha_1 \ .$$

Relations (2.8) and (2.9) yield

$$\tan\Delta\psi = -\frac{1}{\alpha_1} \qquad \text{and} \qquad \sin\Delta\psi = \frac{F}{\sqrt{\beta_1\beta_2}}$$

from which we can conclude the following result: If $\alpha_1 = \alpha_2 = 0$ then, since $\sin\Delta\psi > 0$, we must have $\Delta\psi = \pi/2$ and $F = \sqrt{\beta_1\beta_2}$.

This relation links the lens focal length F and the length $L = 2F$ of the module to the magnitude of the β values.

Practical two-dimensional modules based on this concept are typically achieved by symmetric triplets or by quadruplets, as shown in Fig. 8.

For the triplet, the focal length is different in the two phase planes (x, x') and (y, y') because of basic properties of triplets.

If it is required that $F_x = F_y$, then a symmetric quadruplet array of quadrupoles may be used as illustrated in Fig. 8.

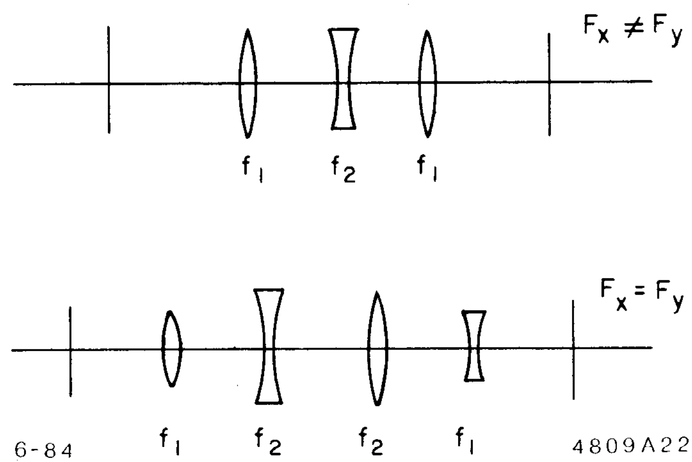

Fig. 8. A Triplet and a Quadruplet Lens System Possessing Parallel to Point and Point to Parallel Imaging in Both Planes.

3.1.2 The FODO Array

The FODO array is perhaps the most common building block used in the design of machine lattices and beam lines. Its structure is illustrated in Fig. 9 when it is composed entirely with quadrupoles. A FODO array with interspersed dipoles is discussed in Ref. 7.

It is informative to study the FODO array at two different observation points in order to better understand its basic properties.

1) <u>First case</u>: The cell begins and ends at the center of a lens, then the transfer matrix for the x and y planes is obtained by the following multiplication:

$$R = \begin{pmatrix} 1 & 0 \\ \mp 1/2f & 1 \end{pmatrix} \begin{pmatrix} 1 & L \\ 0 & 1 \end{pmatrix} \begin{pmatrix} 1 & 0 \\ \pm 1/f & 1 \end{pmatrix} \begin{pmatrix} 1 & L \\ 0 & 1 \end{pmatrix} \begin{pmatrix} 1 & 0 \\ \mp 1/2f & 1 \end{pmatrix}$$

where again the upper sign applies to the (x, x') plane and the lower sign to the (y, y') plane.

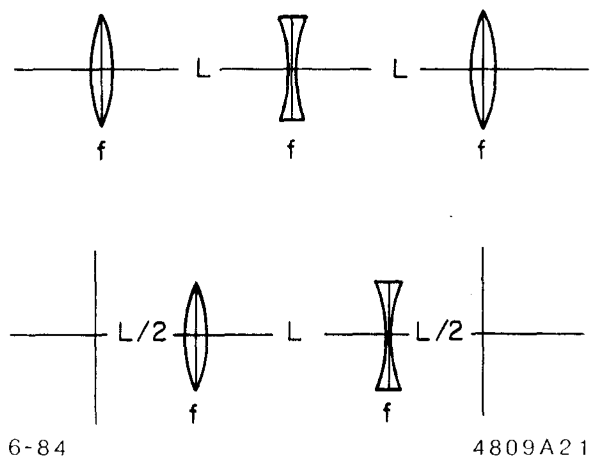

Fig. 9. A FODO Array as a Building Block for Lattices. 1) The Transformation for one Cell between the Centers of the Lenses. 2) The Transformation for one Cell between the Centers of the Drift Regions.

If we assume that $\beta_1 = \beta_2 = \beta$ and $\alpha_1 = \alpha_2 = \alpha$, then

$$R = \begin{pmatrix} c + \alpha s & \beta s \\ -\gamma s & c - \alpha s \end{pmatrix} = \begin{pmatrix} \left(1 - \frac{L^2}{2f^2}\right) & 2L\left(1 \pm \frac{L}{2f}\right) \\ -\frac{L}{2f^2}\left(1 \mp \frac{L}{2f}\right) & \left(1 - \frac{L^2}{2f^2}\right) \end{pmatrix}$$

from which

$$\cos\mu = c = \left(1 - \frac{L^2}{2f^2}\right) ,$$

$$\sin\left(\frac{\mu}{2}\right) = \sqrt{\frac{(1 - \cos\mu)}{2}} = \frac{L}{2f} ,$$

$$\beta_{x,y} = 2L\frac{1 \pm \sin(\mu/2)}{\sin\mu} ,$$

and

$$\alpha_{x,y} = 0 ,$$

Using symmetry arguments, the ratio of the beta functions in the focusing and defocusing lenses is given by

$$\frac{\beta_{\max}}{\beta_{\min}} = \frac{1+\sin(\mu/2)}{1-\sin(\mu/2)} \ .$$

Note that this ratio is independent of the length of the cell.

2) <u>Second case</u>: If we now begin the FODO array in the middle of one of its drifts, the transfer matrix for one cell is given by

$$R = \begin{pmatrix} 1 & L/2 \\ 0 & 1 \end{pmatrix} \begin{pmatrix} 1 & 0 \\ \pm 1/f & 1 \end{pmatrix} \begin{pmatrix} 1 & L \\ 0 & 1 \end{pmatrix} \begin{pmatrix} 1 & 0 \\ \mp 1/f & 1 \end{pmatrix} \begin{pmatrix} 1 & L/2 \\ 0 & 1 \end{pmatrix} \ ;$$

then

$$R = \begin{pmatrix} c+\alpha s & \beta s \\ -\gamma s & c-\alpha s \end{pmatrix} = \begin{pmatrix} \left(1-\dfrac{L^2}{2f^2}\right) \mp \dfrac{L}{f} & 2L - \dfrac{L^3}{4f^2} \\ -\dfrac{L}{f^2} & \left(1-\dfrac{L^2}{2f^2}\right) \pm \dfrac{L}{f} \end{pmatrix}$$

from which we obtain

$$\cos\mu = \left(1-\frac{L^2}{2f^2}\right) \ ,$$

$$\sin\left(\frac{\mu}{2}\right) = \frac{L}{2f} \ ,$$

which is the same as in case 1, but

$$\beta_{x,y} = \frac{L}{\sin\mu}\left(2-\sin^2(\mu/2)\right)$$

and

$$\alpha_{x,y} = \mp\frac{2\sin(\mu/2)}{\sin\mu} \ .$$

The last two relations show that at this location we have the result

$$\beta_x = \beta_y \qquad \text{and} \qquad \alpha_x = -\alpha_y \ ,$$

which is the same property possessed by a thin lens quadrupole.

A case of particular interest is obtained when $\mu = \pi/2$. This corresponds to $(L/f) = \sqrt{2}$. This FODO cell is then often referred to as a 'quarter-wave' or $\lambda/4$ transformer and is shown schematically in Fig. 10.

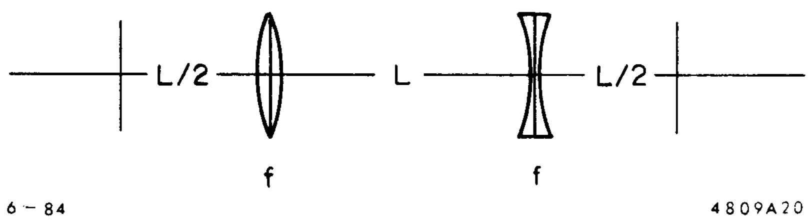

Fig. 10. The $\lambda/4$ Transformer.

The transfer matrix R of this quarter-wave transformer is

$$R_{x,y} = \begin{pmatrix} \mp\sqrt{2} & 3L/2 \\ -2/L & \pm\sqrt{2} \end{pmatrix}$$

and we have the interesting property $R_{11} = -R_{22}$ and R_{11}, and R_{22} both change signs between the x and y planes. This is a useful cell for phase space matching as will be discussed later.

3.1.3 A Telescopic System

The optical system illustrated in Fig. 11 is called telescopic.

Its transfer matrix is given by

$$R = \begin{pmatrix} 1 & F_2 \\ 0 & 1 \end{pmatrix} \begin{pmatrix} 1 & 0 \\ -1/F_2 & 1 \end{pmatrix} \begin{pmatrix} 1 & F_1 + F_2 \\ 0 & 1 \end{pmatrix} \begin{pmatrix} 1 & 0 \\ -1/F_1 & 1 \end{pmatrix} \begin{pmatrix} 1 & F_1 \\ 0 & 1 \end{pmatrix}$$

$$= \begin{pmatrix} -F_2/F_1 & 0 \\ 0 & -F_1/F_2 \end{pmatrix} = \begin{pmatrix} -M & 0 \\ 0 & -1/M \end{pmatrix} . \tag{3.1}$$

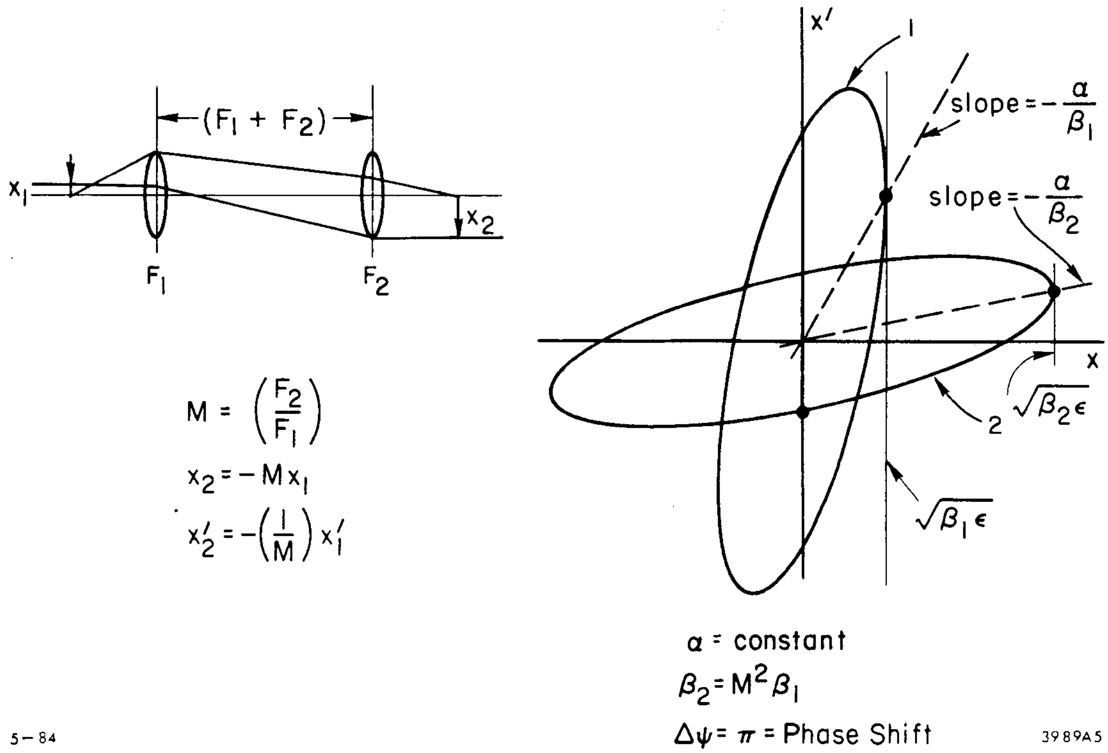

Fig. 11. A one-Dimensional Telescopic System.

From the R matrix we obtain

$$x_2 = -Mx_1 \qquad \text{and} \qquad x_2{}' = -\frac{x_1{}'}{M} \ .$$

The relation (2.7) becomes:

$$\begin{pmatrix} \beta_2 \\ \alpha_2 \\ \gamma_2 \end{pmatrix} = \begin{pmatrix} M^2 & 0 & 0 \\ 0 & 1 & 0 \\ 0 & 0 & 1/M^2 \end{pmatrix} \begin{pmatrix} \beta_1 \\ \alpha_1 \\ \gamma_1 \end{pmatrix}$$

which shows that

$$\beta_2 = M^2\beta_1 \qquad \text{and} \qquad \alpha_2 = \alpha_1 = \text{a constant} \ .$$

Since $R_{12} = 0$, the relations (2.8) and (2.9) reduce to

$$\tan \Delta\psi = 0 \qquad \text{and} \qquad \sin \Delta\psi = 0 \ .$$

Using the formula (2.5) rewritten as

$$R = \begin{pmatrix} \sqrt{\frac{\beta_2}{\beta_1}} \cos \Delta\psi & 0 \\ 0 & \sqrt{\frac{\beta_1}{\beta_2}} \cos \Delta\psi \end{pmatrix}$$

we deduce that $\cos \Delta\psi < 0$, and consequently that $\Delta\psi = \pi$.

A telescopic system has an optical magnification M given by

$$M = \frac{F_2}{F_1} \; .$$

It also has the property that the transfer matrix R is an invariant if a drift length situated to the right of the lenses is transported to the front with the multiplication factor M^2. To prove and illustrate this property, consider the telescopic system having the transfer matrix of Eq. (3.1) and let it be preceded by a drift of length l_1 and followed by a drift of length l_2. The total matrix is

$$\begin{aligned} R_T &= \begin{pmatrix} 1 & l_2 \\ 0 & 1 \end{pmatrix} \begin{pmatrix} -M & 0 \\ 0 & -(1/M) \end{pmatrix} \begin{pmatrix} 1 & l_1 \\ 0 & 1 \end{pmatrix} \\ &= \begin{pmatrix} -M & -Ml_1 - l_2/M \\ 0 & -(1/M) \end{pmatrix} \; . \end{aligned}$$

The matrix R_T is equal to the matrix of the original telescopic system if and only if the following condition holds:

$$Ml_1 + l_2/M = 0$$

or equivalently

$$l_2 = -M^2 l_1 \; .$$

In practice, to achieve a telescope in both planes one needs at least two quadrupoles to simulate each lens of the telescope. Figure 12 shows such a solution.

The magnification may be different in each plane; therefore, the general 4×4 transfer matrix of the system becomes

$$R = \begin{pmatrix} -M_x & 0 & 0 & 0 \\ 0 & -1/M_x & 0 & 0 \\ 0 & 0 & -M_y & 0 \\ 0 & 0 & 0 & -1/M_y \end{pmatrix}$$

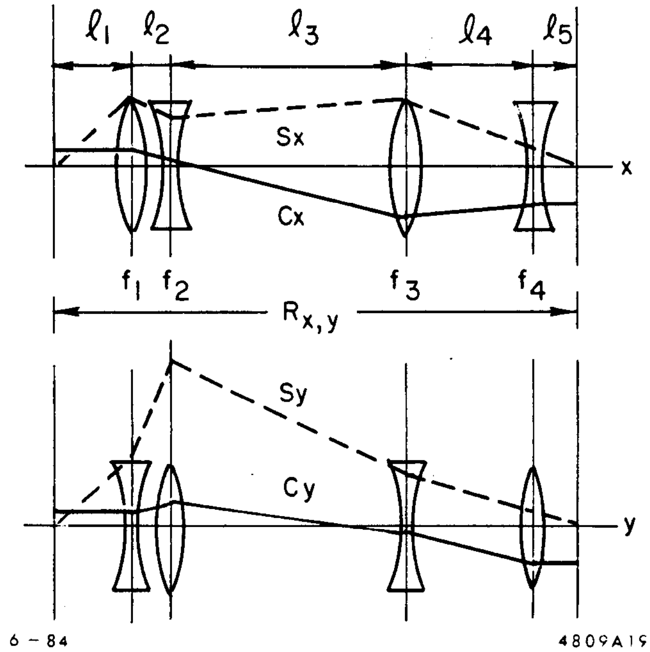

Fig. 12. A two-Dimensional Telescopic System.

or

$$R = \begin{pmatrix} -\sqrt{\dfrac{\beta_{2x}}{\beta_{1x}}} & 0 & 0 & 0 \\ 0 & -\sqrt{\dfrac{\beta_{1x}}{\beta_{2x}}} & 0 & 0 \\ 0 & 0 & -\sqrt{\dfrac{\beta_{2y}}{\beta_{1y}}} & 0 \\ 0 & 0 & 0 & -\sqrt{\dfrac{\beta_{1y}}{\beta_{2y}}} \end{pmatrix} .$$

3.2 Phase Ellipse Matching in Circular Machines

All lattices, be they beamlines or segments of circular machines, are made by the juxtaposition of a series of cells having different transfer properties. One important problem facing the designer can be expressed in the following way:

Consider a section S_2 which is to follow a section S_1. Is it possible to design an intermediate section S_{12} such that S_1 and S_2 are matched? The problem of finding such a section S_{12} is called the section matching problem.

Many design programs help the designer in solving this problem in its generality. It is, however, important to have some rational guidelines on how this matching can be achieved. The following paragraphs indicate two general methods for matching one FODO array to another FODO array or an 'interaction region' to the main lattice of the machine, etc.

3.2.1 General Considerations on FODO Cell Matching

Consider the matched symmetric FODO cell that was described in paragraph 4.1.2. If we choose the beginning of the cell to be halfway between the two quadrupoles, the following conditions hold at this point in every cell:

$$\beta_x = \beta_y \qquad \text{and} \qquad \alpha_x = -\alpha_y \ .$$

Consider now two sets of FODO cells characterized by the two sets of relations

$$\beta_{1x} = \beta_{1y} \qquad \text{and} \qquad \alpha_{1x} = -\alpha_{1y} \ ,$$

$$\beta_{2x} = \beta_{2y} \qquad \text{and} \qquad \alpha_{2x} = -\alpha_{2y} \ .$$

What properties should a matching section have in order to transform the values β_1, α_1, γ_1 into the values β_2, α_2, γ_2? If the transfer matrix of the matching section for the x, x' plane is

$$R = \begin{pmatrix} R_{11} & R_{12} \\ R_{21} & R_{22} \end{pmatrix}$$

then the following relation exists:

$$\begin{pmatrix} \beta_2 \\ \alpha_2 \\ \gamma_2 \end{pmatrix} = \begin{pmatrix} R_{11}^2 & \underline{-2R_{11}R_{12}} & R_{12}^2 \\ \underline{-R_{11}R_{21}} & R_{11}R_{22} + R_{12}R_{21} & \underline{-R_{12}R_{22}} \\ R_{21}^2 & \underline{-2R_{21}R_{22}} & R_{22}^2 \end{pmatrix} \begin{pmatrix} \beta_1 \\ \alpha_1 \\ \gamma_1 \end{pmatrix} \ . \tag{3.2}$$

Let us note the following:

If at the input of the matching cell we have

$$\beta_{1x} = \beta_{1y} \qquad \text{and} \qquad \alpha_{1x} = -\alpha_{1y} \tag{3.3}$$

and if the transfer matrix R of the matching cell is such that the underlined elements in Eq. (3.2) change sign from the (x, x') plane to the (y, y') plane and the other elements do not change sign, then it follows from the Twiss transformation that:

$$\beta_{2x} = \beta_{2y} \qquad \text{and} \qquad \alpha_{2x} = -\alpha_{2y} \ .$$

When such a situation is created, then the phase ellipse values of one FODO cell are matched to the values of another FODO cell. This, however, does not mean that the above procedure matches any FODO cell to another arbitrarily chosen FODO cell. The following procedure will exemplify and extend the preceding one.

The first condition can be realized generally in two ways: either the matrix R is such that

$$R = \begin{pmatrix} \underline{R_{11}} & R_{12} \\ R_{21} & \underline{R_{22}} \end{pmatrix}$$

or it is such that

$$R = \begin{pmatrix} R_{11} & \underline{R_{12}} \\ \underline{R_{21}} & R_{22} \end{pmatrix}$$

where we have underlined the elements that must change sign as one switches from plane (x, x') to plane (y, y'). One example of a practical matching system is the following.

3.2.2 Beam Matching with a Quarter-Wave Transformer

Consider the quarter-wave transformer defined in the FODO array section of paragraph 4.1.2 and illustrated in Fig. 13 .

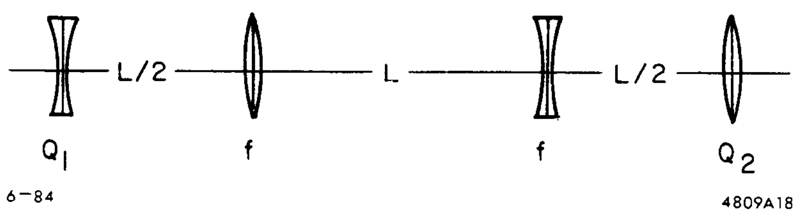

Fig. 13. A Quarter-Wave Matching Transformer.

The matrix element of this cell can be written as

$$R = \begin{pmatrix} \underline{a} & b \\ -c & \underline{-a} \end{pmatrix}$$

where, according to our convention, the underlined elements change sign when switching from the (x, x') plane to the (y, y') plane.

The transformation of this cell satisfies the condition of the previous paragraph, and this cell will match pairs of FODO cells whose parameters both satisfy the relation

$$\begin{pmatrix} \beta_2 \\ \alpha_2 \\ \gamma_2 \end{pmatrix} = \begin{pmatrix} a^2 & \underline{-2ab} & b^2 \\ \underline{ac} & -a^2 - bc & \underline{ba} \\ c^2 & \underline{-2ac} & a^2 \end{pmatrix} \begin{pmatrix} \beta_1 \\ \alpha_1 \\ \gamma_1 \end{pmatrix} .$$

Using the $\lambda/4$ cell, which matches specific pairs of FODO cells, one can obtain, by the addition of two elements, a cell which will match any two pairs of FODO cells (with some constraint on the range of β_2).

Consider a quarter-wave transformer to which we add a quadrupole Q_1 at its entrance and another quadrupole Q_2 at its exit.

The insertion of quadrupole Q_2 does not change the exit value β_2 but will change the value α_2 of the planes (x, x') and (y, y') in opposite directions and so preserves the condition $\alpha_{2x} = -\alpha_{2y}$.

The insertion of quadrupole Q_1 at the entrance does not change the value β_1 or the relation $\alpha_{1x} = -\alpha_{1y}$ but it does change the absolute values of α_{1x} and α_{1y}. The Twiss transformation, Eq. (2.7), for the quarter-wave transformer shows that this variation of Q_1 will change the values of both β_2 and α_2 while preserving the conditions $\beta_{1x} = \beta_{1y}$ and $\alpha_{1x} = -\alpha_{1y}$.

Using the transformation matrix of the quarter-wave transformer and considering α_1 to be variable (via variation of the strength of Q_1), one can show that the value β_2 that can be matched by the preceding cell has a minimum value equal to b^2/β_1, as follows:

The expression for β_2 is

$$\begin{aligned} \beta_2 &= a^2\beta_1 - 2ab\alpha_1 + b^2\gamma_1 \\ &= a^2\beta_1 - 2ab\alpha_1 + \frac{b^2(1+\alpha_1^2)}{\beta_1} . \end{aligned}$$

The first and second derivatives with respect to α_1 are

$$\frac{d\beta_2}{d\alpha_1} = -2ab + \frac{2b^2\alpha_1}{\beta_1}$$

and

$$\frac{d^2\beta_2}{d\alpha_1^2} = \frac{2b^2}{\beta_1} > 0 .$$

Therefore, a minimum will be achieved if

$$\alpha_1 = \frac{a}{b}\beta_1$$

and the value of this minimum is

$$\beta_{2\min} = \frac{b^2}{\beta_1} \ .$$

The procedure of adjustment of the matching cell then becomes:

The quadrupole Q_1 is adjusted so that, given the input values β_1, α_1, the required output value β_2 is achieved at the exit. Quadrupole Q_2 is then adjusted to obtain the required α_2, and the match is accomplished. There are other modules that have similar properties. Information about some of them can be found in Ref. 8.

Sometimes there are situations where it is not possible to install quadrupole Q_1. An example of this might be at the interaction region of a collider. In this case, the quarter-wave matching transformer can still be made to work by choosing the parameter b in the above equations so as to achieve the required output value of β_2 at the exit of the module. Then the quadrupole Q_2 may be adjusted to obtain the required $\alpha_x = -\alpha_y$ at the exit of the transformer.

3.2.3 Matching with Half-Wave Transformers

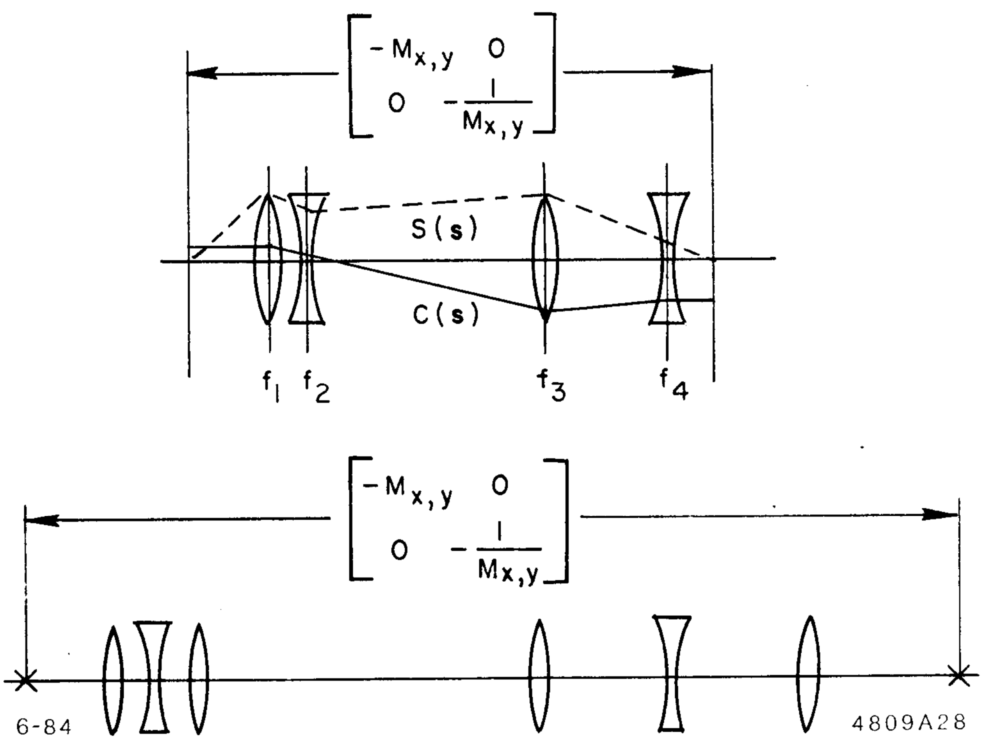

Fig. 14. A Half-Wave Matching Transformer: 1) using Doublets; 2) using Triplets.

Telescopic systems which have a phase shift of π may also be used as matching transformers with the restriction that $\alpha_2 = \alpha_1$ and $\beta_2 = M^2\beta_1$, where M is the optical magnification of the transformer. Their most obvious application is to match between two points where $\alpha_1 = \alpha_2 = 0$ (the location of an erect phase ellipse). They have the advantage that M_x does not have to equal M_y. They also have the property of minimizing the higher-order optical distortions because of their optical symmetry. Examples of half-wave matching transformers are illustrated schematically in Fig. 14.

4 SECOND-ORDER OPTICS MODULES

In TRANSPORT a general notation for the coefficients of the Taylor expansion of the solution of the equations of motion was introduced. The notation of the first-order terms was simplified in order to conform with the standard matrix notation. For example,

$$R_{11} = (x|x_0) \ , \qquad R_{21} = (x'|x_0) \ , \qquad R_{34} = (y|y'_0) \ .$$

In order to ease the writing, a similar simplification of notation was introduced for the second-order terms: the tensor T_{ijk} can be defined in a similar way. For example,

$$T_{112} = (x|x_0x'_0) \ , \qquad T_{246} = (x'|y'_0\delta) \ .$$

All terms for which no subscript is equal to 6 will be referred to as geometric aberrations because they depend only upon the central momentum p_0.

Any term where one subscript is equal to 6 will be referred to as a chromatic aberration by virtue of the fact that its effect depends on the momentum deviation $\delta = \Delta p/p_0$ of the particle.

4.1 Chromatic Corrections using the -I Module

Chromatic effects occur because particles with different momenta respond differently to a given magnetic field. Consider two FODO cells in repetitive sequence tuned so that $\mu_{x,y} = 90$ degrees for each cell. Such a setup is often referred to as a $-I$ telescopic transformer because its transfer matrix in both the x and y transverse planes is

$$R_{x,y} = -I = \begin{pmatrix} -1 & 0 \\ 0 & -1 \end{pmatrix} \ .$$

The same would be true for three 60 degree cells, etc.

In Fig. 15 is a schematic representation of such a $-I$ transformer. Let 1 and 2 denote the entrance and exit positions.

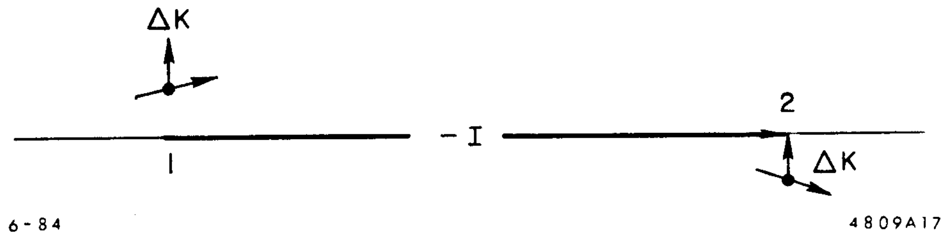

Fig. 15. Principle of a $-I$ transformer.

A particle at position 1 with coordinates x_1, x_1' will emerge at position 2 with coordinates x_2, x_2' given by

$$x_2 = -x_1 \qquad \text{and} \qquad x_2' = -x_1' \ .$$

Imagine now that we place at position 1 a thin magnetic element that produces an angle kick to the particle, say ΔK. The particle of momentum p_0 will now arrive at position 2 with the coordinates

$$x_2 = -x_1 \qquad \text{and} \qquad x_2' = -x_1' - \Delta K \ .$$

If we now submit the particle to another angle kick equal to ΔK at position 2, we see that the exit coordinates are the same as they were without kicks. In conclusion, when particles are submitted to equal angle kicks at the entrance and exit points of a $-I$ transformer, there is no visible effect on their behavior outside the $-I$ transformer for monoenergetic particles having momentum p_0.

Let us apply this principle, using some of our elementary building blocks.

1) Dipoles: Dipoles are even-order elements in the sense that the angle kick they deliver to a particle is an even function of the lateral displacement (in this case a constant function). Thus, if we place two identical dipole magnets (one at the entrance and one at the exit) of a $-I$ transformer, there will be no net angular deflection experienced by particles of momentum p_0 outside of the $-I$ transformer and the total system will be achromatic to first-order.

2) Quadrupoles: The angular displacement produced by a quadrupole is an odd function of the lateral position x. (In this case the angle kick is proportional to x.) Consequently two identical quadrupoles of opposite polarity placed at the entrance and exit of a $-I$ transformer will have no net geometric effect outside the transformer.

3) Sextupoles: Sextupoles are even-order elements . The angular kick they produce is proportional to x^2. In this instance pairs of equal strength sextupoles will have no net geometric effect outside the $-I$ transformer.

Thus, in summary, all odd-order elements (quadrupoles, octupoles, etc.) will have to be introduced in pairs of opposite polarity, and all even-order elements (dipoles, sextupoles, etc.) have to be introduced in pairs with the same polarity in order for the geometric cancellation to be effective.

4.1.1 A $-I$ Transform Sextupolar Chromatic Correction section

Consider now a $-I$ transformer with two sextupoles of equal strength placed at the entrance and exit, and suppose that dipoles have been inserted in each cell of the $-I$ transformer. From the previous discussion we know that the sextupoles will not introduce second-order geometric aberrations. The presence of the dipoles between the sextupoles ensures that there will be coupling between the sextupole strengths and the chromatic behavior of particles. Having thus demonstrated the principle of the chromatic correction, let us analyze its feasibility in greater detail.

In practice one must do at least one chromatic correction per phase plane, and sometimes two or more per plane. The ideal situation, from the point of view of the second-order geometric aberrations, is to assemble enough $-I$ transformers so that the different sextupole pairs (placed $-I$ apart) do not interfere with each other.[9] This condition is often prohibitive in its space requirement and in its cost. So let us analyze the effect of interlacing sextupole pairs used in chromatic corrections.

Consider, as shown in Fig. 16, two consecutive $-I$ transformers containing two interlaced pairs of sextupoles S_1 and S_2.

If the sextupoles are pure second-order elements, no additional second-order aberrations are introduced by the coupling between the sextupoles of the two pairs.

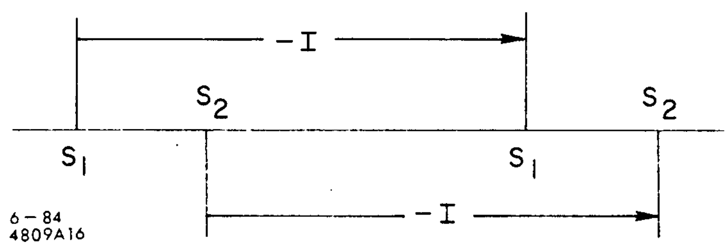

Fig. 16. Interlaced Sextupole Pairs.

Suppose a particle arrives at the first sextupole S_1 with displacement x_1. As it reaches the first sextupole of the pair S_2, its motion, within the $-I$ transformer that separates the pair S_1, is perturbed, and the particle will reach the second sextupole of the S_1 pair with a displacement that is not equal to $-x_1$. Consequently the second sextupole of the S_1 pair will not exactly compensate the geometrics introduced by the the first sextupole. However since the disturbance introduced by the sextupole S_2 is of order two, the uncorrected geometric aberration of the pair S_1 is of order three and four.

In a following paragraph we shall show a complete practical setup of a correction scheme using interlaced families of sextupoles.

4.2 Geometric Correction Using Repetitive Symmetry

The second-order geometric aberrations are obtained by the computation of integrals containing the sinelike and cosinelike functions from TRANSPORT theory. We know that symmetries introduced in the design of a lattice may have the desirable effect of canceling some aberrations.[10] The important symmetry to be considered here is the repetitive symmetry.

Let us look at a general approach to the study of the effect of this symmetry on the second-order aberrations.

Second-order geometric aberration terms can be expressed as

$$T_{ijk} = \int_0^L K_p(R_{ij}(s))^n(R_{ik}(s))^m ds \qquad \text{where} \qquad (n+m) = 3$$

where K_0 is the dipole strength per unit length and K_2 is the sextupole strength per unit length, see Ref. 2. Pure quadrupoles do not generate second-order geometric aberrations so K_1 is not important for this discussion.

Since the $R_{ij}(s)$ are linear combinations of $\sin \Delta\psi$ and $\cos \Delta\psi$, we can write

$$T_{ijk} = \int_0^L F_p \sin^n(\Delta\psi)\cos^m(\Delta\psi) ds$$

where the functions F_p are equal to the strengths K_p multiplied by some power of the $\beta(s)$ functions. Adopting a complex variable notation, we obtain the condition for having all second-order geometric terms T_{ijk} vanish, namely,

$$\int_0^L F_p e^{\pm i\psi} ds = 0 \qquad \text{and} \qquad \int_0^L F_p e^{\pm 3i\psi} ds = 0 \ .$$

The integral of the expressions $F_p e^{\pm i\psi}$ and $F_p e^{\pm 3i\psi}$ for each separate element of a lattice can be represented geometrically as a vector in the complex plane, as shown in Fig. 17. The integrals over the total lattice become the vector sums of all the complex vectors representing the geometric aberrations of the individual elements, namely,

$$\sum_{1}^{N} F_k e^{i\psi_k} \qquad \text{and} \qquad \sum_{1}^{N} F_k e^{3i\psi_k} \; .$$

For reasons that should appear clear in the next paragraph, one generally places the vectors corresponding to $i\psi$ in one diagram and the vectors corresponding to $3i\psi$ in another. The second-order geometric aberrations are zero if both these sums are zero.

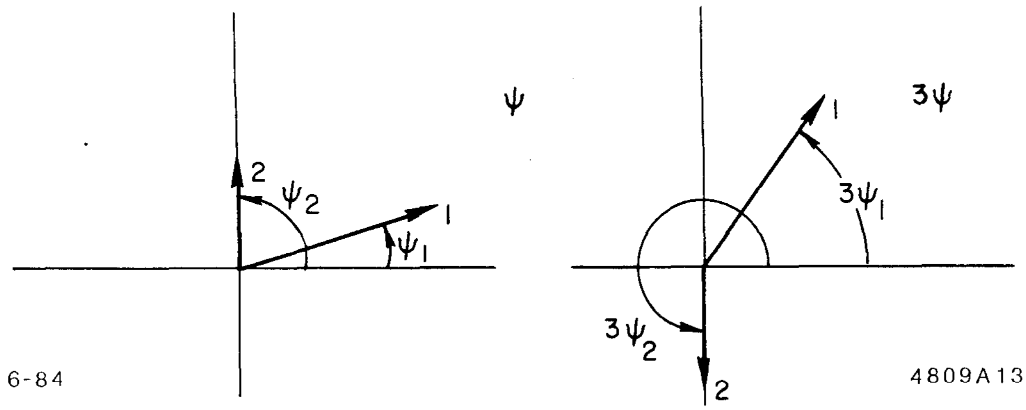

Fig. 17. Complex Plane Diagram for Second-Order Geometric Aberrations.

For repetitive symmetry (i.e. when the lattice is made of a sequence of equal cells), the beta functions are equal from cell to cell and so are the element strengths.

In this case the functions $F_p(s)$ are equal in value at the same location from cell to cell. Let us analyze two special cases: a lattice containing four identical cells and a lattice containing three identical cells, and such that the total phase advance for the lattice is 2π in both cases.

Consider the ψ plot of Fig. 18. The vectors correspond to the number of the cell to which they belong. In the ψ plane they appear in consecutive order with an angle of 90 degrees. Their sum obviously is zero. In the 3ψ plane the angle between consecutive vectors becomes 270 degrees, and their sum will also be zero.

In conclusion, in a lattice made of four equal cells with total phase shift of 2π, the second-order geometric aberrations originating in individual elements will cancel.

Consider now the ψ plot of Fig. 19. The three vectors display an angle of 120 degrees, and so their sum is also zero. However, in the 3ψ plot they will have an angle of 360 degrees and will all coincide. Their sum is not zero unless their amplitude is zero.

In conclusion, for a lattice with three cells and a total phase shift of 2π, some geometric aberrations do not cancel.

We can now formulate the following important theorem:

In a lattice made of n identical cells with $n > 3$ and having a total phase shift of $2m\pi$, all second-order geometric aberrations will cancel.

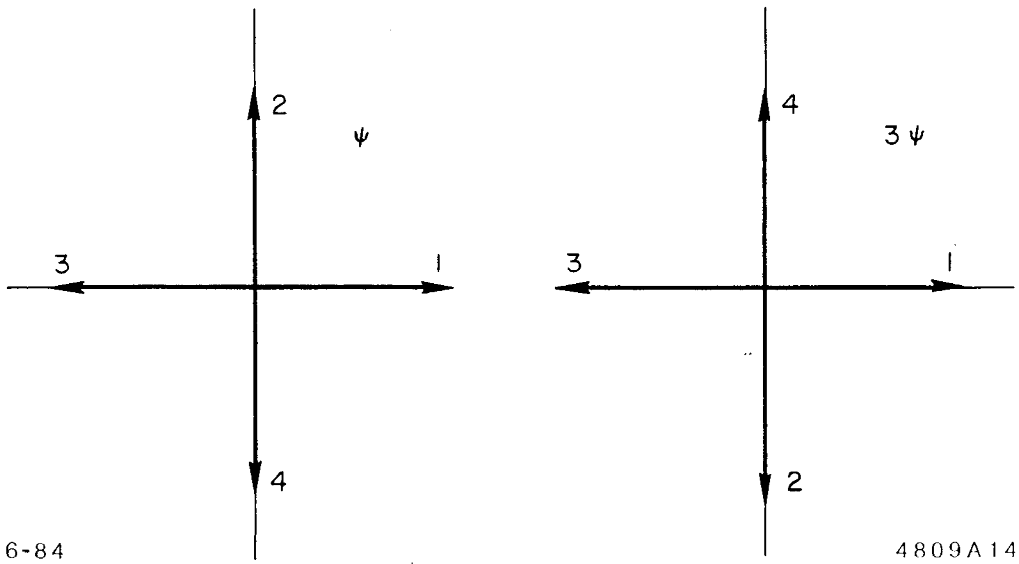

Fig. 18. Complex Plane Diagram for Second-Order Aberrations in a Four-Cell Lattice with Repetitive Symmetry and a 2π Phase Shift.

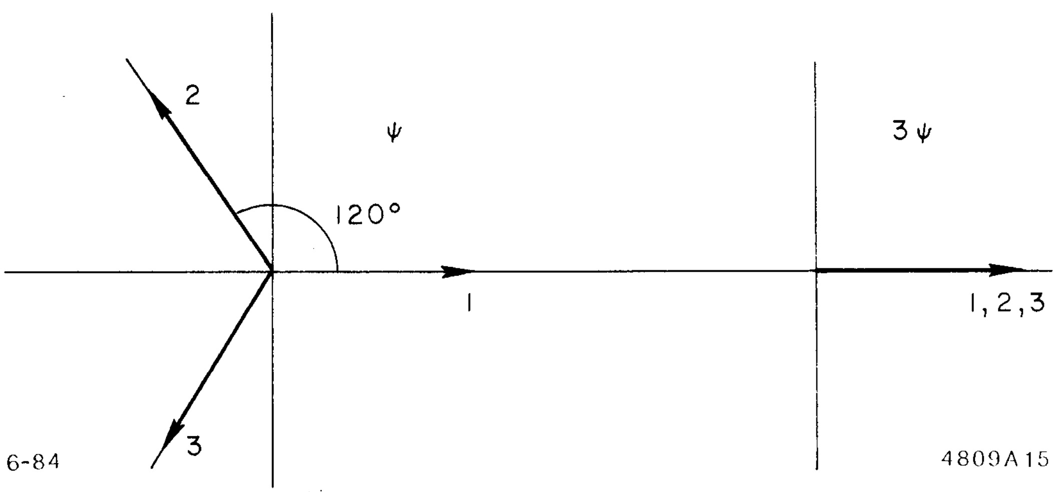

Fig. 19. Complex Plane Diagram for Second-Order Aberrations in a Three-Cell Lattice with Repetitive Symmetry and a 2π Phase Shift.

4.2.1 *The First-Order Achromat*

Consider a lattice made of n identical cells having the following transfer matrix:

$$R = \begin{pmatrix} a & b & u \\ c & d & v \\ 0 & 0 & 1 \end{pmatrix} = \begin{pmatrix} M & \vec{w} \\ 0 & 1 \end{pmatrix} .$$

The total transfer matrix T will be

$$T = \begin{pmatrix} M^n & M^{n-1}\vec{w} + M^{n-2}\vec{w} + \cdots + \vec{w} \\ 0 & 1 \end{pmatrix} .$$

The dispersive vector of the total transfer matrix T can be written in the following form:

$$\vec{d} = (M^{n-1} + M^{n-2} + \cdots + I)\vec{w} = (M^n - I)(M - I)^{-1}\vec{w} .$$

From the above expression one can deduce the following theorem:

A lattice made of n identical cells is achromatic to first order if and only if

1) $M^n = I$

or

2) $\vec{w} = 0$.

In other words, it is achromatic if and only if each cell is achromatic, or the total transfer matrix is the identity matrix (equivalently if the total phase advance is $2m\pi$ for any integer m).

This first-order result is the basis for the building of second-order achromatic beam lines.

4.2.2 *A Practical Second-Order Achromat*

Figure 20 shows a possible layout for a four-cell second-order achromat. The labels BD stand for bending dipoles. The labels QF and QD stand for horizontally focusing quadrupoles and horizontally defocusing quadrupoles. We assume that the quadrupoles have been tuned to provide a total phase advance of 2π.

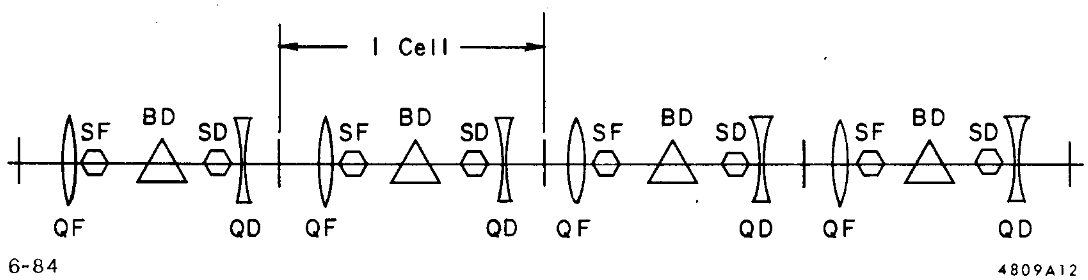

Fig. 20. Example of a Practical Second-Order Achromat with Four Cells.

Sextupoles have been introduced so that the chromatic correction procedure can be performed in both the (x, x') and the (y, y') plane.

The sextupoles of the family SF will couple predominantly with the x plane because they are located close to the focusing quadrupoles, where the values of the β_x function are greater.

Similarly the sextupoles of the family SD will couple predominantly to the y motion, where β_y is larger.

Once the quadrupoles have been tuned to provide a 2π phase shift, the second-order geometric aberrations introduced by the dipoles and by the sextupoles cancel exactly.

One then tunes the sextupoles SF and SD so that one of the second-order chromatic terms T_{1j6} or T_{2j6} and one of T_{3j6} or T_{4j6} are zero. It has been shown previously[11] that all the second-order chromatic terms except T_{566} then become simultaneously zero.

We now have a system that is completely achromatic to second order with the only exception being the momentum dependence of the path length.

4.2.3 Application of the Achromat Concept to Chromatic Corrections

The second-order achromat as described above is an optical system whose transformation matrix is the identity matrix to a precision of second order in all of the phase space variables x, x', y, y', l, and δ except for the matrix elements for the path length which depenmd only upon δ . These are R_{56} and T_{566}.

While the second-order achromat may not be directly applicable to the design of circular machines, the optical principles evolved for its development are definitely useful when formulating the sextupole configurations necessary for the chromatic corrections in circular machines and in particular for storage rings, where the interaction regions have very small beta functions. Let us review the salient features of the second-order correction theory developed above that are applicable to this problem.

1) Any family of sextupoles inserted into a lattice such that their vector sums cancel in the ψ and 3ψ diagrams described above will not introduce second-order geometric aberrations.

2) The interlacing of two or more sextupole families, each of which satisfies criterion 1), does not introduce second-order geometric aberrations.

3) Interlacing of one sextupole family with another sextupole family will introduce third- and higher-order distortions to the lattice.

4) It should be noted that in order for the sextupoles not to introduce second-order geometric distortions, the tune shift per cell of the lattice in the region of the sextupoles must remain fixed. The quadrupoles in this region must not be used to vary the tune of the machine. The variation in tune must be achieved in a 'sextupole-free' region.

In summary we may state the following theorems :

Theorem A : One of the important principles of the second-order achromat is the following: "If one combines four or more identical cells consisting of dipole, quadrupole, and sextupole components, with the parameters chosen so that the overall first-order transfer matrix is equal to unity (+I) in both transverse planes, then it follows that such a system will have vanishing second-order geometric (on momentum) aberrations".

Theorem B : Furthermore, "If the sextupole components are adjusted so as to make one second-order chromatic aberration vanish in each transverse plane of the +I sections, then ALL second-order aberrations (geometric, chromatic and path length) will vanish except for the path length matrix elements depending only upon δ .

Theorem A is useful for making chromatic corrections in particle accelerators such as storage rings and linear colliders where low beta sections are used for the interaction regions. For these applications, it is sometimes referred to as a "pseudoachromat".

The entire achromat, using both theorems A and B, is useful for the design of secondary beams or for the transport of primary beams , such as in the arcs of the Stanford Linear Collider, where optical distortions must be kept to a minimum.

The property of the second-order achromat, whereby dipole and sextupole families may be inserted into a lattice for chromatic corrections without introducing second-order geometrical (on momentum) optical distortions, has been incorporated in several new particle accelerator designs. These include the SLC at SLAC, LEP at CERN, the EROS pulstretcher ring at SASKATOON, the CEBAF ring at SURA and the MIT ring.[12]

REFERENCES

1. K.L. Brown, A First and Second-Order Matrix Theory for the Design of Beam Transport Systems and Charged Particle Spectrometers, SLAC Report No. 75, or Advances in Particle Physics. 1,71-134 (1967).
2. K.L. Brown and R.V. Servranckx, First and Second Order Charged Particle Optics, SLAC-PUB-3381 (July 1984).
3. K.L. Brown, D.C. Carey, Ch. Iselin and F. Rothacker, TRANSPORT a Computer Program for Designing Charged Particle Beam Transport Systems, SLAC 91 (1973 rev.), NAL 91, and CERN 80-04.
4. H. Bruck, Accelerateurs Circulaires de Particules. Presses Universitaires de France, Paris (1966).
5. E.D. Courant and H.S. Snyder, Theory of the Alternating Gradient Synchrotron, Annals of Physics, Vol. 3, 1-48 (1958).
6. C. Bovet et al., A Selection of Formulae and Data Useful for the Design of A. G. Synchrotrons, CERN/MPS-SI/Int. DL/70/4 April, 1970.
7. R.V. Servranckx, Circular Machine Design Techniques and Tools, presented at this Conference.
8. K.L. Brown, Beam Envelope Matching for Beam Guidance Systems, SLAC-PUB-2370 (August 1980), and Nucl. Instrum. and Methods 187 (1981) 51-65; Presented at the Conference on charged particle optics, Giessen, West Germany, September 8-12, 1980.
9. K.L. Brown and R.V. Servranckx, Chromatic Corrections for Large Storage Rings, the 11th International Conference on High Energy Accelerators, CERN, Geneva, Switzerland, 1980, p. 656-660.
10. K.L. Brown, A Second-Order Magnetic Optical Achromat, SLAC-PUB-2257 (February 1979), and IEEE Transactions on Nuclear Science, Vol NS-26, No. 3, June 1979, p. 3490-3492.
11. D.C. Carey, Why a Second-Order Magnetic Optical Achromat Works, FERMILAB PUB 79/61-EXP, 2042, and Nucl. Instrum. and Methods 189 (1981) 365-367.
12. K.L. Brown and R.V. Servranckx, Applications of the Second-Order Achromat Concept to the Design of Particle Accelerators. 1985 Particle Accelerator Conference, Vancouver, BC, Canada, May 13-16, 1985, pp. 2288-2290.